



Halogenated hydrocarbon gas sensing by rotational absorption spectroscopy in the 220–330 GHz frequency range

T. E. Rice¹ · M. A. Z. Chowdhury¹ · M. W. Mansha² · M. M. Hella² · I. Wilke³ · M. A. Oehlschlaeger¹

Received: 28 January 2021 / Accepted: 6 July 2021 / Published online: 2 August 2021
© The Author(s), under exclusive licence to Springer-Verlag GmbH Germany, part of Springer Nature 2021

Abstract

Gas sensing for halogenated hydrocarbons is demonstrated using rotational absorption spectroscopy in the 220–330 GHz frequency range, carried out with a compact and robust broadband microelectronics-based THz-wave spectrometer. Monitoring of halogenated hydrocarbons is necessary in industrial situations where these chemicals present a danger to human health and the environment, due to their toxicity, volatility, and reactivity. The absorption spectra for pure chloromethane, dichloromethane, chloroform, iodomethane, and dibromomethane were characterized at 297 K and pressures from 0.25 to 16 Torr. The spectra show the unique rotational fingerprints for the target halogenated hydrocarbons in the 220–330 GHz frequency range and demonstrate the potential for their selective quantitative detection in gas sensing applications with minimum detection for pure gases of order 10^{12} – 10^{13} molecules/cm³ and for dilute gases of order 10–100 ppm at 1 atm for a 1 m pathlength. The study further demonstrates the potential of all-electronic miniaturized THz-wave gas sensors.

1 Introduction

The detection and identification of gas-phase halogenated hydrocarbons is of interest in industrial monitoring, process control and optimization, and environmental remote sensing applications. Polar molecules, such as halogenated hydrocarbons, have unique rotational spectra which offer opportunity for the development of non-intrusive gas sensing technologies using absorption spectroscopy in the THz wave frequency range (0.1–10 THz) [1–7].

Absorption spectroscopy and gas sensing using THz frequency electromagnetic waves is mostly impervious to scattering by airborne particles because THz wavelengths (~ 1 mm in the current study) are large compared to the typical sizes of airborne particles (0.01–100 μm). In view of industrial gas sensing in the field, this is an advantage of

THz waves in comparison with shorter wavelengths bands of the electromagnetic spectrum (e.g., infrared, near-infrared) where scattering of electromagnetic waves by airborne particles is intrinsically stronger.

Interference of THz wave absorption measurements by atmospheric water vapor is reduced compared to infrared absorption measurement because water vapor absorption lines are sparse in the THz frequency band, compared to the infrared frequency band, particularly below 1 THz. In the current frequency band of interest, water vapor has only one distinct and weak transition.

These advantages of THz wave absorption spectroscopy, together with recent progress in microelectronic THz wave sources and detectors, make possible the development of low power, miniaturized, robust gas sensor systems for industrial and environmental remote sensing of halogenated hydrocarbons by exploiting the unique rotational spectral features of these molecules in the THz frequency band. THz wave gas sensing technologies have been demonstrated in trace gas detection in human breath [8, 9], cigarette smoke [10], volatile organic compounds (VOCs) [7], and other applications [11]. However, prior development of THz wave absorption sensors based on microelectronics technologies for halogenated hydrocarbons are limited.

Sensitive gas sensor systems for halogenated hydrocarbons are important because these industrial chemicals pose a severe risk to humans, due to their toxicity and volatility,

✉ T. E. Rice
ricet4@rpi.edu

¹ Department of Mechanical, Aerospace and Nuclear Engineering, Rensselaer Polytechnic Institute, Troy, NY, USA

² Department of Electrical, Computer and Systems Engineering, Rensselaer Polytechnic Institute, Troy, NY, USA

³ Department of Physics, Applied Physics and Astronomy, Rensselaer Polytechnic Institute, Troy, NY, USA

and are well-known to deplete stratospheric ozone, even at extremely low concentrations due to their catalytic properties [12, 13]. Chlorinated hydrocarbons are particularly important in stratospheric ozone destruction, with chloromethane (CH_3Cl), the simplest chlorinated hydrocarbon, present at only 600 ppt in the atmosphere but, yet, having contributed to as much as 15–16% of the depletion of the ozone layer [13–15]. Atmospheric chloromethane originates from both natural and anthropogenic sources, including the biosynthesis of fungi, algae, and other plant organisms, forest fires, coal combustion, and combustion of vegetation and biomass [16–20]. Over the past 20 years, although anthropogenic emissions of chloromethane have subsided, chloromethane is still used as a solvent in the production of rubbers, polymers, polyurethane foams, surfactants, pesticides, pharmaceuticals and can be released to the atmosphere in these processes [21].

Dichloromethane (CH_2Cl_2), an unregulated industrial solvent that is considered a short-lived compound in the atmosphere (residence time of less than 6 months), is increasing in atmospheric concentration rapidly due to increased anthropogenic emissions from its use in the foam cleaning of metals of other materials [22–24] and from natural processes such as biomass fires [25]. Chloroform (CHCl_3) is a colorless, sweet-smelling hazardous chlorinated hydrocarbon with a well-known profound effect on the human nervous system, inducing dizziness at small exposures and leading to organ damage at high exposures [26]. Chloroform has been historically used as an anesthetic and a refrigerant. While its use for these purposes has greatly declined, chloroform is still produced in large quantities as a precursor to polytetrafluoroethylene (PTFE), for producing dyes and pesticides, and as a solvent in the pharmaceutical industry [27].

Iodinated and brominated hydrocarbons, industrial chemicals, also play a role in the depletion of stratospheric ozone, including iodomethane (methyl iodide, CH_3I) [28, 29]. Due to its uses as a fumigant and pesticide, iodomethane, carcinogenic and toxic, can leach into groundwater and contaminate soil [30]. Finally, a great portion of the Antarctic ozone depletion from the late 1980s to the 2000s has been attributed to stratospheric bromine [31, 32], for which dibromomethane (CH_2Br_2), an industrial solvent and reactant in organic synthesis processes [33], is a key source [34].

The present study reports on the potential for the gas sensing of halogenated hydrocarbons in the 220–330 GHz frequency range using absorption spectroscopy and radiation generation and detection via microelectronic sources. The study presents an extension of our previous work on gas sensing for oxygenated hydrocarbon VOCs [7]. We specifically focus on the detection of six halogenated hydrocarbons that are important in industrial and environmental processes:

chloromethane, dichloromethane, chloroform, iodomethane, diiodomethane, and dibromomethane.

2 Experimental setup and methodology

Absorption spectra in the 220–330 GHz frequency range were measured using the hardware and methods developed in Rice et al. [7], where the experiment is comprised of an amplitude-modulated microelectronics source, based on frequency multiplication of RF input, gas cell, and Schottky diode detector. The spectral absorption of gas samples was measured using the Beer–Lambert law:

$$A = \epsilon cl = -\ln\left(\frac{I}{I_0}\right),$$

where A is the absorbance, ϵ the absorption coefficient, c the concentration of the absorbing gas, l the pathlength, I the transmitted intensity of the radiation after absorption, and I_0 the reference intensity (no absorption). The gas cell pathlength, l , for the experiments conducted here was 0.22 m. However, for the estimation of detection limits (results section), a standard pathlength of 1.0 m was used, where detection limits are inversely proportional to pathlength and can be adjusted for any desired pathlength. The absorption coefficient varies with frequency, temperature, pressure, and gas mixture composition, through the contribution of the line intensities and shapes for each transition. To measure an absorption spectrum, we first record the reference intensity by sweeping the radiation source in frequency space while the gas cell is under vacuum. Next, the cell is filled with the gas of interest to a desired pressure, the radiation source is swept again in frequency, the transmitted intensity is recorded, and the Beer–Lambert law is used to convert the measured intensities to absorbance. In both cases, the intensity signals are demodulated DC signals from the lock-in amplifier. The final absorbance signal processed with a low-pass filter with a cutoff frequency of 300 Hz to increase the signal-to-noise. The resulting absorption spectrum has a noise floor of ± 0.001 to ± 0.003 in absorbance and a frequency resolution of 15 MHz. Signals from an example experiment are shown in Fig. 1.

3 Results and discussion

Measurements of spectral absorbance have been made in the 220–330 GHz frequency range for five pure halogenated hydrocarbons at room temperature (297 K) and the pressures shown in Table 1. Reagent grade chemicals (Sigma–Aldrich) with natural isotopic composition were used at purity levels

Fig. 1 Example experiment carried out for pure chloromethane at 0.5 Torr and 297 K. Top and middle graphs: modulated reference (I_0 , black) and transmitted (I , blue) intensities as measured at the detector (top graph shows full frequency range and middle graph a subset); bottom graph: absorbance within a subset of the frequency range at 261–266 GHz (color figure online)

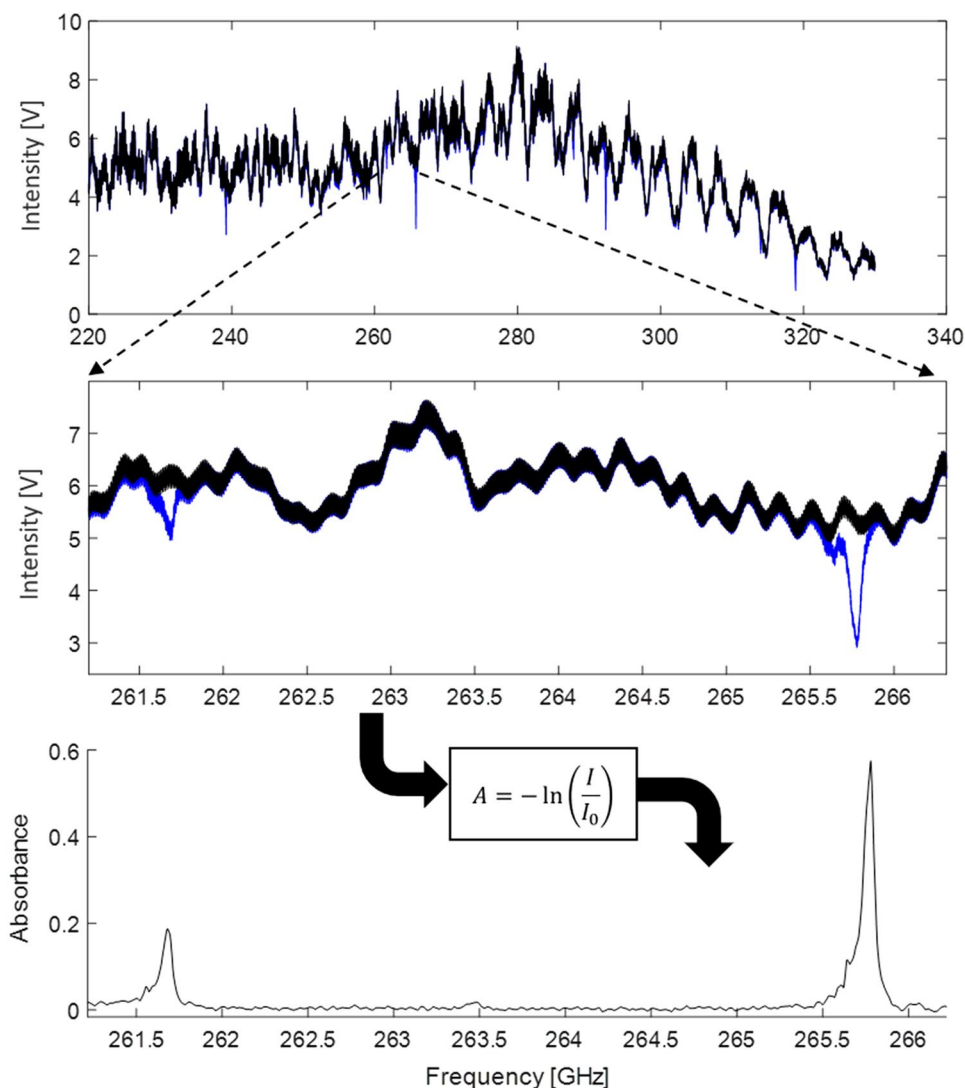


Table 1 Compounds and pressures at which spectral absorption measurements were performed (1 Torr = 133.322 Pa)

Compound	Molecular formula	Pressures [Torr]
Chloromethane (methyl chloride)	CH ₃ Cl	0.25, 0.5, 1, 2, 4, 8
Iodomethane (methyl iodide)	CH ₃ I	0.5, 1, 2, 4, 8, 16
Dichloromethane (methylene chloride)	CH ₂ Cl ₂	0.5, 1, 2, 4
Dibromomethane (methylene bromide)	CH ₂ Br ₂	0.5, 1, 2, 4, 8, 16
Chloroform (trichloromethane)	CHCl ₃	0.5, 1, 2, 4

of > 99% to > 99.8%. Example measured spectra are found in the figures within this section and a complete set of all measurements can be found in the appended supplementary material.

Absorption spectra for chloromethane are shown in Figs. 2 and 3. In the present frequency range, chloromethane shows very four strong features for each of the two primary isotopomers (¹²CH₃³⁵Cl and ¹²CH₃³⁷Cl with natural abundance of 74.9% and 23.9%, respectively).

Chloromethane, a symmetric top molecule, has well-quantified rotational spectroscopy [35], with rotational energy levels that can be given as:

$$E_{J,K} = BJ(J+1) + (A-B)K^2 - D_J(J(J+1))^2 - D_{J,K}J(J+1)K^2 - D_KK^4, \quad (1)$$

where J and K are the rotational quantum numbers, A and B rotational constants, and D_J , $D_{J,K}$ and D_K centrifugal distortion

Fig. 2 Spectral absorption measurements for pure chloromethane at 2 Torr. Note, features for two isotopologues are observed and the rotational quantum numbers for each transition are identified

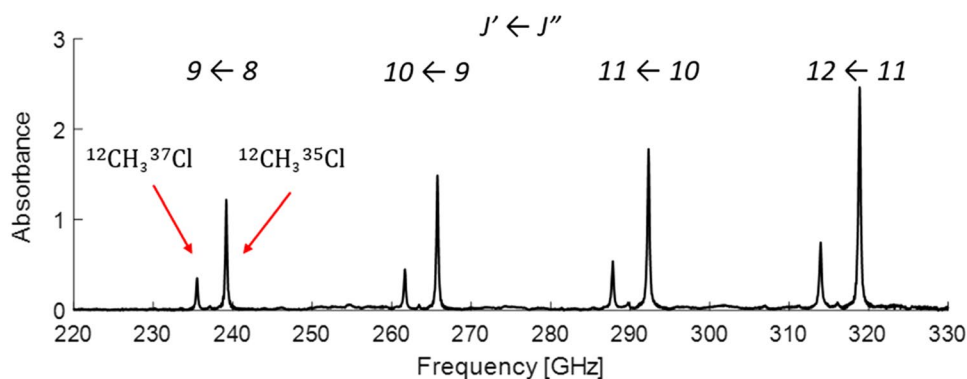
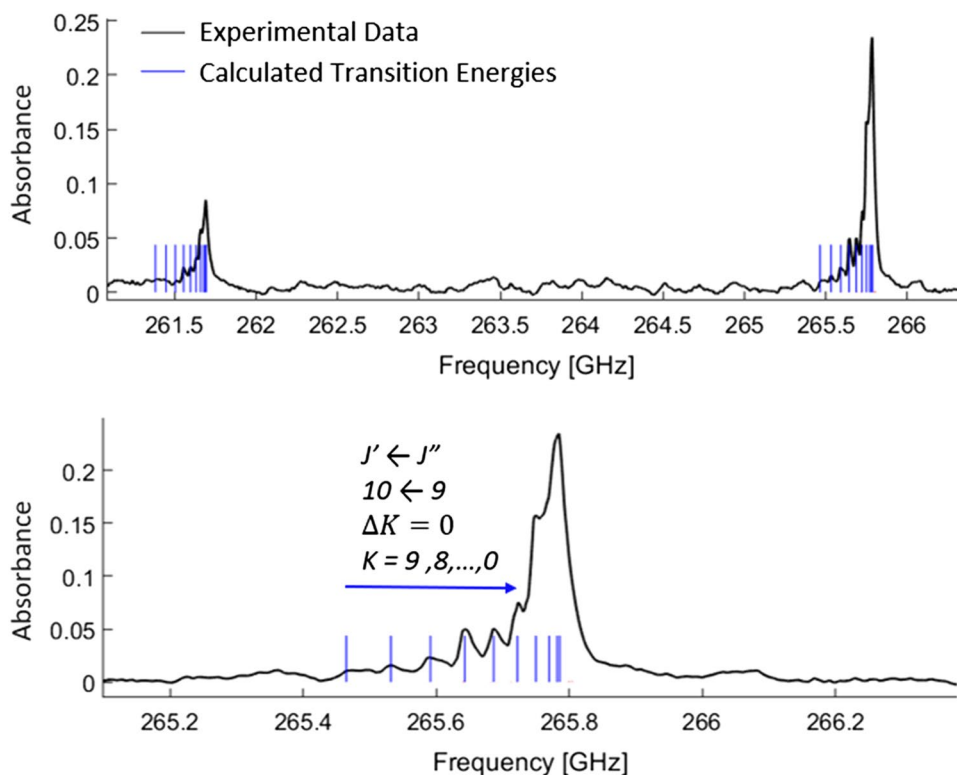


Fig. 3 Measured absorption spectra for pure chloromethane at 0.25 Torr in the 261–266 GHz range. Calculated rotational transition frequencies are shown via the blue lines



terms. Within Fig. 2, the frequencies of rotational transitions predicted by Eq. 1 and the rotational spectroscopic constants reported by Striteska et al. [35] are indicated by the blue lines and are in good agreement with the JPL molecular spectroscopy database [36]. The strong features observed in Fig. 2 obey the symmetric top selection rules, $J' = J'' + 1 \leftarrow J''$ and $\Delta K = 0$, and are located at frequencies given by:

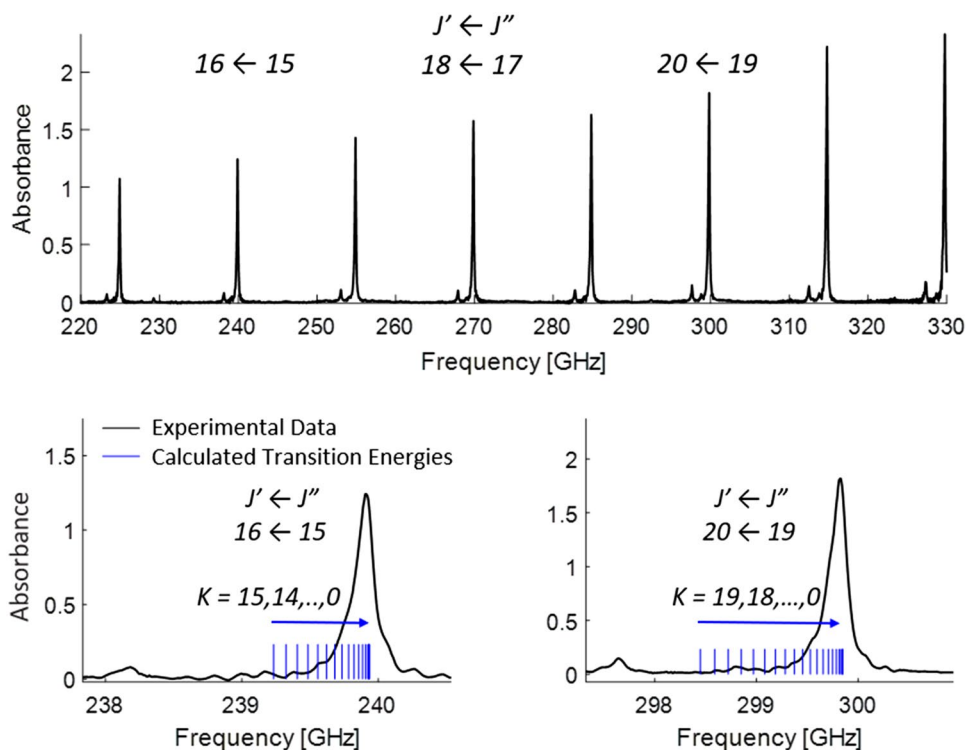
$$\Delta E_{J,K} = 2B(J'' + 1) - 4D_J(J''^3 + 3J''^2 + 3J'' + 4) - 2D_{JK}(J'' + 1)K^2$$

Hence, these features are approximately spaced in frequency every $2B$, where the rotational constants are

$A = 156.052$ GHz and $B = 13.293$ GHz for $^{12}\text{CH}_3^{35}\text{Cl}$, and $A = 156.053$ GHz and $B = 13.088$ GHz for $^{12}\text{CH}_3^{37}\text{Cl}$. Within these major features, distinct rotational structure is resolved, as shown in Fig. 3, caused by centrifugal distortion (D_J and $D_{J,K}$ terms).

Iodomethane displays absorption within the spectral region that is similar to chloromethane, as shown in Fig. 4. Iodomethane, also a symmetric top, has strong repeating absorption features spaced every $2B$, where the rotational constants are $A = 155.095$ GHz and $B = 7.501$ GHz [37], following symmetric top selection rules: $J' = J'' + 1 \leftarrow J''$ and $\Delta K = 0$. Again, multiple distinct transitions originate near the location of each major feature due to centrifugal

Fig. 4 Measured absorption spectrum for pure iodomethane at 0.5 Torr. Blue lines indicate calculated frequencies for transitions (color figure online)

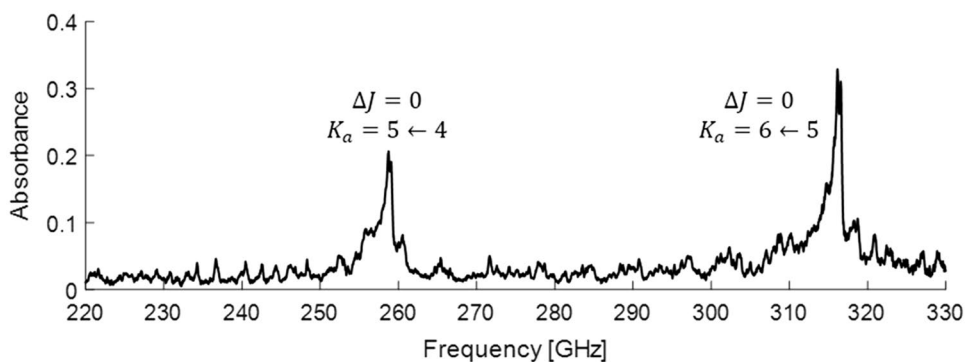


distortion. In the case of iodomethane, these features are more closely spaced than for chloromethane and are not well resolved experimentally. The calculated frequency locations based on the rotational constants reported by Boucher et al. [37] are also shown in Fig. 4 in blue and are in agreement with the experiment. Weak absorption features that are separated from the strongest features are also observed in the iodomethane spectrum. These features originate from the small fractions of iodomethane that populate the first vibrationally excited state at room temperature. Similar weak features from vibrationally excited chloromethane are also observed in Figs. 2 and 3 at frequencies between the peaks for the two chloromethane isotopomers.

An example measured spectrum for dichloromethane is shown in Fig. 5. Dichloromethane is a near-prolate ($\kappa = -0.98$) asymmetric top with three primary isotopomers:

$\text{CH}_2^{35}\text{Cl}_2$ (natural abundance 56%; rotational constants $A = 32.002$ GHz, $B = 3.320$ GHz, $C = 3.065$ GHz [38]); $\text{CH}_2^{35}\text{Cl}^{37}\text{Cl}$ (abundance 38%; $A = 31.879$ GHz, $B = 3.231$ GHz, $C = 2.988$ GHz [38]); and $\text{CH}_2^{37}\text{Cl}_2$ (abundance 6%). The dichloromethane spectrum in the present frequency range is dominated by Q -branch b -type transitions that blend together at frequencies around 258 and 315.5 GHz and obey the selection rules: $\Delta J = 0, \pm 1$; $\Delta K_a = \pm 1$; $\Delta K_c = \pm 1$, where J is the quantum number for total rotational angular momentum and K_a and K_c are the quantum labels for projection of total angular momentum onto the a - and c -axes, respectively. The strong feature at 258 GHz is for $\Delta J = 0$ and $K_a' = 5$ $K_a'' = 4$ and the strong feature at 315.5 GHz is for $\Delta J = 0$ and $K_a' = 6$ $K_a'' = 5$. For each strong feature, there is a sequence of lines for each K_a'' at a spacing of $(B + C)$ for $\Delta J = \pm 1$ transitions. The slightly different

Fig. 5 Measured absorption spectrum for pure dichloromethane at 2 Torr



rotational constants for the three chloromethane isotopomers contribute to the asymmetry of the strong features at 258 and 315.5 GHz, with the transitions for $\text{CH}_2^{35}\text{Cl}^{37}\text{Cl}$ and $\text{CH}_2^{37}\text{Cl}_2$ shifted to lower frequencies, and the numerous weak lines between these strong features.

The spectral absorption for dibromomethane in the current frequency range, example shown in Fig. 6, is similar to that for dichloromethane. Dibromomethane is also a near-prolate ($\kappa > 0.99$) asymmetric top with multiple isotopomers: $\text{CH}_2^{79}\text{Br}_2$ (natural abundance 26%; rotational constants $A=26.035$ GHz, $B=1.239$ GHz, $C=1.191$ GHz [39]); $\text{CH}_2^{79}\text{Br}^{81}\text{Br}$ (abundance 50%; rotational constants $A=26.008$ GHz, $B=1.223$ GHz, $C=1.177$ GHz [40]); and $\text{CH}_2^{81}\text{Br}_2$ (abundance 24%; rotational constants $A=25.998$ GHz, $B=1.208$ GHz, $C=1.163$ GHz [39]). Like dichloromethane, the dibromomethane spectrum

contains strong Q -branch b -type transitions near 223, 272, and 332 GHz that correspond to $\Delta J=0$ and $\Delta K_a = +1$, where $K_a''=5$ (223 GHz), $K_a''=6$ (272 GHz), and $K_a''=7$ (322 GHz). Similarly, the subsequent transitions that follow these major transitions are for $\Delta J = +1$ and $\Delta = +1$. The transitions for the present isotopomers are clustered close enough together such that they reside within and coalesce into one apparent peak in the absorbance spectrum.

An example measured spectra for chloroform is shown in Fig. 7. Chloroform has four primary isotopomers that are oblate or near-oblate symmetric tops: $\text{CH}^{35}\text{Cl}_3$ (natural abundance 42.9%; rotational constants $A=B=3.302$ GHz, $C=1.778$ GHz [41]); $\text{CH}^{35}\text{Cl}_2^{37}\text{Cl}$ (natural abundance 42%; rotational constants $A=3.302$ GHz, $B=3.187$ GHz, $C=1.683$ GHz [42]); $\text{CH}^{35}\text{Cl}^{37}\text{Cl}_2$ (natural abundance 13.7%; rotational constants $A=3.244$ GHz, $B=3.129$ GHz,

Fig. 6 Measured absorption spectrum measurements for pure dibromomethane at 2 Torr

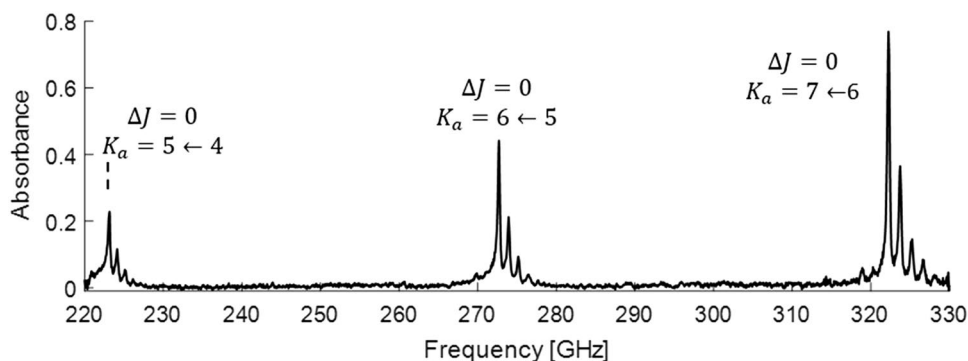
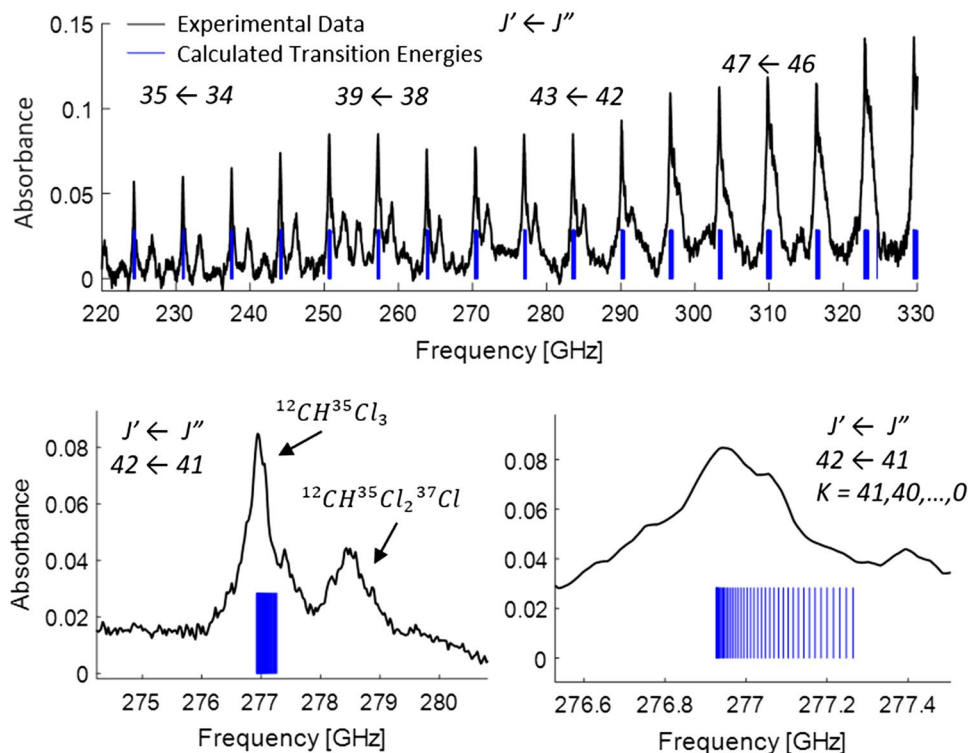


Fig. 7 Measured absorption spectra for pure chloroform at 4 Torr. Blue lines indicate features that result from R-branch transitions for $\text{CH}^{35}\text{Cl}_3$. The secondary peak at a slightly higher frequency is from the $\text{CH}^{35}\text{Cl}^{37}\text{Cl}_2$ isotopic species of chloroform, based on the rotational constants reported by Colmont et al. [42] (color figure online)



$C = 1.77842$ GHz [42]); and $\text{CH}^{37}\text{Cl}_3$ (natural abundance 1.5%). The chloroform spectrum in the current frequency region contains strong repeating transitions that are identifiable for the three most abundant isotopomers as *R*-branch transitions, $\Delta J = +1$, and are spaced in frequency at $A + B$. The spectrum shown in Fig. 7 indicates the locations of transitions for $\text{CH}^{35}\text{Cl}_3$. The spectral features located between the labeled features for $\text{CH}^{35}\text{Cl}_3$ can be assigned to the other isotopomers. Note, at high frequencies the transitions for isotopomers blend together due to their proximity and collisional lineshape broadening.

Measured absorption spectra for all five compounds studied are compared in Fig. 8. It is evident that there are distinct and strong spectral features allowing for the quasi-isolated simultaneous selective identification of each species in the presence of other species from this subset of halogenated hydrocarbons. For the chlorinated hydrocarbons (top graph in Fig. 8), chloromethane is sufficiently well isolated and

strongly absorbing at the peaks located around 266, 293, and 319 GHz for detection at those locations. Similarly, dichloromethane can be detected at peaks for its broad features located around 259 and 316 GHz. Chloroform provides weaker absorption but has peaks that are sufficiently isolated for detection around 251, 270, and 291 GHz. The strong features around 272 and 322 GHz for dibromomethane (middle graph in Fig. 8) allow for its selective measurement in the presence of any other absorber for the selected halogenated hydrocarbons. Finally, iodomethane (bottom graph in Fig. 8) has a number of strong and isolated spectral features, starting at around 225 GHz and repeating approximately every 15 GHz, allowing its detection in the presence of any of the other compounds.

The strong absorption features observed in the 220–330 GHz frequency range allow for sensitive detection of the five target halogenated hydrocarbons, at detection limits suitable for industrial gas sensing. Assuming a minimum

Fig. 8 Comparison of measured absorption spectra for halogenated hydrocarbons at 297 K. Top graph: chloromethane at 0.25 Torr, dichloromethane at 2 Torr, and chloroform at 4 Torr. Middle graph: dichloromethane at 1 Torr and dibromomethane at 0.5 Torr. Bottom graph: chloromethane and iodomethane at 0.5 Torr

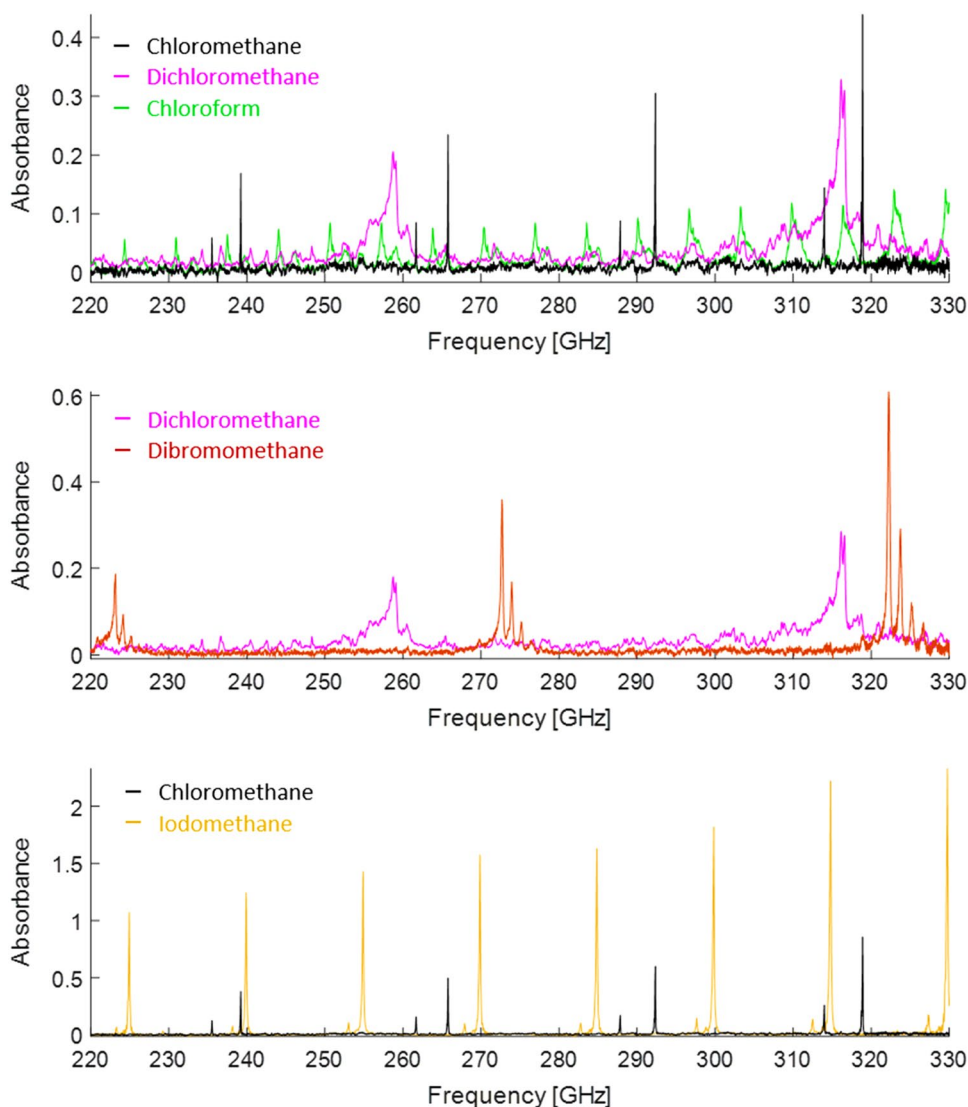


Table 2 Gas-phase detection and exposure limits for target halogenated hydrocarbon species (297 K and 1 m absorption pathlength)

Compound	Detection frequency [GHz]	Estimated detection limits		Exposure limits
		Pure gas concentration [cm^{-3}]	Dilute gas concentration at 1 atm	
Chloromethane, CH_3Cl	319	4×10^{12}	13 ppm	TWA: 100 ppm (OSHA) C: 200 ppm
Iodomethane, CH_3I	300	2×10^{12}	7 ppm	TWA: 2 ppm (OSHA)
Dichloromethane, CH_2Cl_2	316	2×10^{13}	70 ppm	TWA: 25 ppm (cal/OSHA) ST: 125 ppm
Dibromomethane, CH_2Br_2	322	6×10^{12}	20 ppm	TWA: 25 ppm (NIH) ST: 125 ppm
Chloroform, CHCl_3	291	5×10^{13}	180 ppm	TWA: 2 ppm (OSHA) C: 50 ppm

TWA: time weighted average exposure limit (8 h), ST: short-term exposure limit (15 min), and C: ceiling exposure limit

detectible absorbance, the concentration limits for pure gas detection of the five target compounds at chosen detection frequencies can be estimated from the present data set. In the present study, for a single frequency sweep with amplitude modulation but no averaging, absorbance noise ranges from ± 0.001 to ± 0.003 . By averaging multiple sweeps or decreasing the sweep rate (or range) the absorbance noise can be reduced well below ± 0.001 . Hence, for the purposes of determining detection limits, we will use a minimum detectible absorbance of ± 0.001 which yields the estimated detection limits for the measurement of pure halogenated hydrocarbons ranging from order 10^{12} to 10^{13} molecules/ cm^3 , as reported in Table 2. For mixtures of the target halogenated hydrocarbons dilute in a bath gas (e.g., air, N_2 , or He), lineshape broadening will affect the minimum detectible concentrations. The estimated detection limits for dilute gases provided in Table 2 are based on spectral lineshapes which are modeled using pressure broadening parameters extrapolated from calculations for chloromethane [43]. Note, while the absorption pathlength in the present experiment was 21.59 cm, for relevance to other sensor applications, the detection limits are reported for a 1 m pathlength. Detection limits are inversely proportional to pathlength.

4 Conclusions

Rotational spectroscopy on gaseous halogenated hydrocarbons is demonstrated using an amplitude-modulated all electronic terahertz-source/detector system operating in the 220–330 GHz frequency range. Absorption spectra for pure chloromethane, iodomethane, dichloromethane, dibromomethane, and chloroform are characterized in this frequency range for 297 K and modest pressures (0.25–16 Torr) where collisional lineshape broadening effects are important. The measurements illustrate strong and distinct absorption for the target halogenated hydrocarbon species allowing

for their selective measurement at detection limits suitable for industrial gas sensing applications, where halogenated hydrocarbons present a human health and environmental hazard. The present work further demonstrates the potential of THz-wave microelectronics and rotational absorption spectroscopy for quantitative gas sensing.

Supplementary Information The online version contains supplementary material available at <https://doi.org/10.1007/s00340-021-07667-w>.

Acknowledgements This work was supported by the National Science Foundation under Grant No. CBET-1851291.

References

1. R.M. Smith, M.A. Arnold, *Anal. Chem.* **87**, 10679 (2015)
2. Y.-D. Hsieh, S. Nakamura, D.G. Abdelsalam, T. Minamikawa, Y. Mizutani, H. Yamamoto, T. Iwata, F. Hindle, T. Yasui, *Sci. Rep.* **6**, 28114 (2016)
3. Y. Yang, A. Shutler, D. Grischkowsky, *Opt. Express* **19**, 8830 (2011)
4. S.L. Drexheimer, *Terahertz Spectroscopy Principles and Applications* (CRC Press, Boca Raton, 2008)
5. A. Tekawade, T.E. Rice, M.A. Oehlschlaeger, M.W. Mansha, K. Wu, M.M. Hella, I. Wilke, *Appl. Phys. B* **124**, 105 (2018)
6. M.W. Mansha, K. Wu, T.E. Rice, M.A. Oehlschlaeger, I. Wilke, M.M. Hella, *IEEE Sensors J.* **21**(4), 4553–4562 (2020)
7. T.E. Rice, M.W. Mansha, M.A.Z. Chowdhury, M.M. Hella, I. Wilke, M.A. Oehlschlaeger, *Appl. Phys. B* **126**, 1 (2020)
8. N. Rothbart, O. Holz, R. Koczulla, K. Schmalz, H.W. Hübers, *Sensors (Switzerland)* **19**, 1 (2019)
9. I. R. Medvedev, R. Schueler, J. Thomas, O. Kenneth, H.-J. Nam, N. Sharma, Q. Zhong, D. J. Lary, and P. Raskin, 2016 41st International Conference on Infrared, Millimeter, and Terahertz Waves (IRMMW-THz)
10. D. Bigourd, A. Cuisset, F. Hindle, S. Matton, R. Bocquet, G. Moutet, F. Cazier, D. Dewaele, H. Nouali, *Appl. Phys. B* **86**, 579 (2007)
11. C.F. Neese, I.R. Medvedev, G.M. Plummer, A.J. Frank, C.D. Ball, F.C. De Lucia, *IEEE Sensors J.* **12**, 2565 (2012)

12. R. Hossaini, M.P. Chipperfield, S.A. Montzka, A.A. Leeson, S.S. Dhomse, J.A. Pyle, *Nature Comm.* **8**, 15962 (2017)
13. M.A.K. Khalil, R.A. Rasmussen, *Atmos. Environ.* **33**, 1305 (1999)
14. T. Vannelli, A. Studer, M. Kertesz, T. Leisinger, *Appl. Environ. Microbiol.* **64**, 1933 (1998)
15. L. J. Carpenter, S. Reimann, J. B. Burkholder, C. Clerbaux, B. D. Hall, R. Hossaini, J. C. Laube, and S. A. Yvon-Lewis, Update on ozone-depleting substances (ODSs) and other gases of interest to the Montreal protocol. Scientific assessment of ozone depletion (2014)
16. D.B. Harper, *Biochem. Soc. Trans.* **22**(4), 1007–1010 (1994)
17. A. McCulloch, M.L. Aucott, C.M. Benkovitz, T.E. Graedel, G. Kleiman, P.M. Midgley, Y.F. Li, *J. Geophys. Res. Atmos.* **104**, 8391 (1999)
18. P. Chaignaud, M. Morawe, L. Besaury, E. Kröber, S. Vuilleumier, F. Bringel, S. Kolb, *ISME J.* **12**, 2681 (2018)
19. J.M. Lobert, W.C. Keene, J.A. Logan, R. Yevich, *J. Geophys. Res. Atmos.* **104**, 8373 (1999)
20. L. Derendorp, A. Wishkerman, F. Keppler, C. McRoberts, R. Holzinger, T. Röckmann, *Chemosphere* **87**, 483 (2012)
21. S. Li, M.K. Park, C.O. Jo, S. Park, *J. Atmos. Chem.* **74**, 227 (2017)
22. R. Hossaini, M.P. Chipperfield, S.A. Montzka, A. Rap, S. Dhomse, W. Feng, *Nat. Geosci.* **8**, 186 (2015)
23. P. G. Simmonds, A. J. Manning, D. M. Cunnold, A. McCulloch, S. O'Doherty, R. G. Derwent, P. B. Krummel, P. J. Fraser, B. Dunse, L. W. Porter, R. H. J. Wang, B. R. Grealley, B. R. Miller, P. Salamah, R. F. Weiss, and R. G. Prinn, *J. Geophys. Res.* **2006**, Res. Atmos. [Doi: https://doi.org/10.1029/2006JD007082](https://doi.org/10.1029/2006JD007082)
24. M.L. Cox, G.A. Sturrock, P.J. Fraser, S.T. Siems, P.B. Krummel, S. O'Doherty, *J. Atmos. Chem.* **45**, 79 (2003)
25. M. A. K. Khalil, Reactive chlorine compounds in the atmosphere. In: Reactive halogen compounds in the atmosphere, (Springer, Berlin, Heidelberg, 1999), p. 45–79
26. R.V. Branchflower, D.S. Nunn, R.J. Highet, J.H. Smith, J.B. Hook, L.R. Pohl, *Toxicol. Appl. Pharmacol.* **72**, 159 (1984)
27. P.M. Perillo, D.F. Rodríguez, *Sens. Actuators B Chem.* **193**, 263 (2014)
28. C.D. Odowd, J.L. Jimenez, R. Bahreini, R.C. Flagan, J.H. Seinfeld, K. Hämerl, L. Pirjola, M. Kulmala, T. Hoffmann, *Nature* **417**, e632 (2002)
29. R.J. Huang, K. Seitz, J. Buxmann, D. Pöhler, K.E. Hornsby, L.J. Carpenter, U. Platt, T. Hoffmann, *Atmos. Chem. Phys.* **10**, 4823 (2010)
30. M. Guo, S. Gao, *J. Environ. Qual.* **38**, 513 (2009)
31. R.J. Salawitch, M.B. McElroy, J.H. Yatteau, S.C. Wofsy, M.R. Schoeberl, L.R. Lait, P.A. Newman, K.R. Chan, M. Loewenstein, J.R. Podolske, S.E. Strahan, M.H. Proffitt, *Geophys. Res. Lett.* **17**, 561 (1990)
32. B.M. Sinnhuber, M.P. Chipperfield, S. Davies, J.P. Burrows, K.U. Eichmann, M. Weber, P. Von Der Gathen, M. Guirlet, G.A. Cahill, A.M. Lee, J.A. Pyle, *Geophys. Res. Lett.* **27**, 3473 (2000)
33. D. Yoffe, R. Frim, S. D. Ukeles, M. J. Dagani, H. J. Barda, T. J. Benya, and D. C. Sanders 2000 Bromine compounds. *Ullmann's Encyclopedia of Industrial Chemistry*, 1–31
34. A. Mellouki, R.K. Talukdar, A.-M. Schmoltner, T. Gierczak, M.J. Mills, S. Solomon, A.R. Ravishankara, *Geophys. Res. Lett.* **19**, e2059 (1992)
35. L.N. Štríteská, M. Šimečková, P. Kania, P. Musil, L. Kolesníková, J. Koubek, Š. Urban, *J. Mol. Struct.* **919**, 89 (2009)
36. H.M. Pickett, R.L. Poynter, E.A. Cohen, M.L. Delitsky, J.C. Pearson, H.S.P. Müller, *J. Quant. Spectro. Rad. Trans.* **60**, 883 (1998)
37. D. Boucher, J. Burie, D. Dangoisse, J. Demaison, A. Dubrulle, *Chem. Phys.* **29**, 323 (1978)
38. F. Tullini, G.D. Nivellini, M. Carlotti, B. Carli, *J. Mol. Spectro.* **138**, 355 (1989)
39. D. Chadwick, D.J. Millen, *Trans. Faraday Soc.* **67**, 1539 (1971)
40. Y. Niide, H. Tanaka, I. Ohkoshi, *J. Mol. Spectro.* **139**, 11 (1990)
41. J.H. Carpenter, P.J. Seo, D.H. Whiffen, *J. Mol. Spectro.* **170**, 215 (1995)
42. J.M. Colmont, D. Priem, P. Dréan, J. Demaison, J.E. Boggs, *J. Mol. Spectro.* **191**, 158 (1998)
43. A.S. Dudaryonok, N.N. Lavrentieva, J.V. Buldyreva, *J. Quant. Spectro. Rad. Trans.* **130**, 321 (2013)

Publisher's Note Springer Nature remains neutral with regard to jurisdictional claims in published maps and institutional affiliations.